JOC Article
pubs.acs.org/joc

A Systematic Study of Thermochromic Aromatic Donor−Acceptor Materials

Paul M. Alvey,[†] Joseph J. Reczek,[‡] Vincent Lynch,[†] and Brent L. Iverson*[,†]

[†]*Department of Chemistry and Biochemistry, The University of Texas at Austin, Texas 78712, United States, and* [‡]*Department of Chemistry and Biochemistry, Denison University, Granville, Ohio 43023, United States*

biverson@mail.utexas.edu

Received August 11, 2010

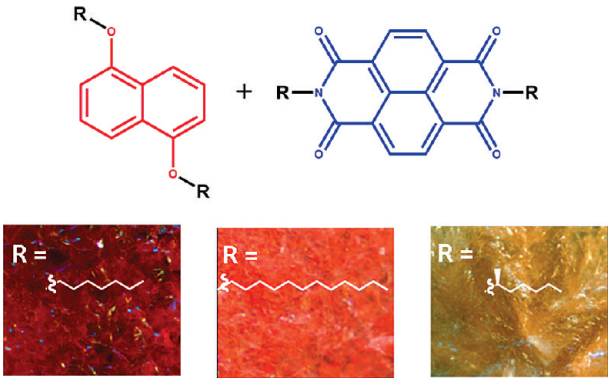

Molar mixtures (1:1) of electron-rich dialkoxynapthalene (Dan) and electron-deficient 1,4,5,8-napthalenetetracarboxylic diimide (Ndi) derivatives form highly tunable, columnar mesophases with a dark red color due to a charge transfer absorbance derived from alternating face-centered stacking. Certain Dan−Ndi mixtures undergo a dramatic color change from dark red to an almost colorless material upon crystallizing from the mesophase. Macroscopic morphology of the solid is not changed during this process. In order to investigate the origins of this interesting thermochromic behavior, Dan and Ndi side chains were systematically altered and their 1:1 mixtures were studied. We have previously speculated that the presence or absence of steric interactions due to side chain branching on the aromatic units controlled the level of color change associated with crystallization. Results from the present study further refine this conclusion including a key crystal structure that provides a structural rationale for the observed results.

Introduction

The assembly of molecules in *solution* via stacking of electron-deficient (acceptor) and electron-rich (donor) aromatic units has proven to be a versatile tool for affecting 2D and 3D molecular architecures.[1−3] The *solid-state* assembly of donor−acceptor complexes has also been achieved through cocrystallization, grinding, and spin-coating techniques.[4] In addition, well-defined macromolecular assemblies have been constructed using bulk blends of either individual or covalently linked liquid crystalline donor−acceptor components.[5] Liquid crystalline mixtures of donor−acceptor molecules offer a high degree of phase tunability relative to single component

(1) (a) Gabriel, G. J.; Sorey, S.; Iverson, B. L. *J. Am. Chem. Soc.* **2005**, *127*, 2637–2640. (b) Bradford, V. J.; Iverson, B. L. *J. Am. Chem. Soc.* **2008**, *130*, 1517. (c) Lokey, R. S.; Iverson, B. L. *Nature* (*London*) **1995**, *375*, 303. (d) Cubberly, M. S.; Iverson, B. L. *J. Am. Chem. Soc.* **2001**, *123*, 7560–7563. (e) Gabriel, G. J.; Iverson, B. L. *J. Am. Chem. Soc.* **2002**, *124*, 15174–15175.

(2) For examples, see: (a) Wang, X.-Z.; Jiang, X.-K.; Li, Z.-T. *Youji Huaxue* **2004**, *24* (7), 753–760. (b) Zhao, X.; Jia, M.-X.; Jiang, X.-K.; Wu, L.-Z.; Li, Z.-T.; Chen, G.-J. *J. Org. Chem.* **2004**, *69*, 270–279. (c) Zhou, Q.-Z.; Jiang, X.-K.; Shao, X.-B.; Chen, G.-J.; Jia, M.-X.; Li, Z.-T. *Org. Lett.* **2003**, *5*, 1955. (d) De, S.; Ramakrishnan, S. *Macromolecules* **2009**, *42* (22), 8599–8603. (e) Colquhoun, H. M.; Zhu, Z.; Cardin, C. J.; Gan, Y.; Drew, M. G. B. *J. Am. Chem. Soc.* **2007**, *129* (51), 16163–16174. (f) Saraogi, I.; Hamilton, A. D. *Chem. Soc. Rev.* **2009**, *38* (6), 1726–1743. (g) Zhou, Q.-Z.; Jia, M.-X.; Shao, X.-B.; Wu, L.-Z.; Jiang, X.-K.; Li, Z.-T.; Chen, G.-J. *Tetrahedron* **2005**, *61*, 7117–7124. (h) Vignon, S. A.; Jarrosson, T.; Iijima, T.; Tseng, H.-R.; Sanders, J. K.; Stoddart, J. F. *J. Am. Chem. Soc.* **2004**, *126*, 9884–9885. (i) Alcalde, E.; Pérez-García, L.; Ramos, S.; Stoddart, J. F.; White, A. J. P.; Williams, D. J. *Chem.—Eur. J.* **2007**, *13*, 3964–3979.

(3) For reviews of aromatic interactions, see: (a) Waters, M. L. *Curr. Opin. Chem. Biol.* **2002**, *6*, 736. (b) Hunter, C. A.; Lawson, K. R.; Perkins, J.; Urch, C. J. *J. Chem. Soc., Perkin Trans. 2* **2001**, 651–669. (c) Hunter, C. A.; Sanders, J. K. M. *J. Am. Chem. Soc.* **1990**, *112*, 5525–5534.

Published on Web 10/25/2010 DOI: 10.1021/jo101498b

systems[6,5c] and may possess enhanced and interesting optoelectronic properties.[7,8] A prominent example using aromatic donor and acceptor liquid crystals involves the assembly of linear charge-transfer (CT) channels,[9] and mesophase columns of segregated donor and acceptor molecules have been proposed as promising structures for organic photovoltaic applications.[10]

We have previously reported that 1:1 molar mixtures of appropriately derivatized electron-rich 1,5-dialkoxynapthalene (Dan) and electron-deficient 1,4,5,8-naphthalenetetracarboxylic diimide (Ndi) units form mesophases over moderate temperature ranges.[6a] These mixtures exhibited dark red isotropic and mesomorphic phases and often dark red crystalline phases as well. The dark red color was attributed to a Dan-Ndi charge transfer absorbance due to the columnar face-centered stacks of alternating Dan and Ndi units. The presence of alternating Dan-Ndi stacks was further supported by polarized optical microscopy, UV−vis spectroscopy, and X-ray powder diffraction studies. An interesting feature of the donor−acceptor stacks of Dan and Ndi units is that attached side chains orient in orthogonal directions. Possibly for this reason, it proved possible to predict and thus fine-tune mesophase transition temperatures through side chain manipulation.[6a] In particular, the isotropic-mesophase transition correlated well with the Ndi side chain identity, while the mesophase-crystalline phase transition temperature correlated well with the Dan side chain identity. One series of mixtures underwent an instantaneous and dramatic color change from dark red to an almost colorless off-white upon crystallization, suggesting a loss of face-centered Dan-Ndi stacking. X-ray powder diffraction studies indicated that the Dan and Ndi components in this series separated into individual microdomains during the crystallization process. Herein is reported a series of systematic studies that further explore this interesting thermochromic behavior of Dan-Ndi materials.

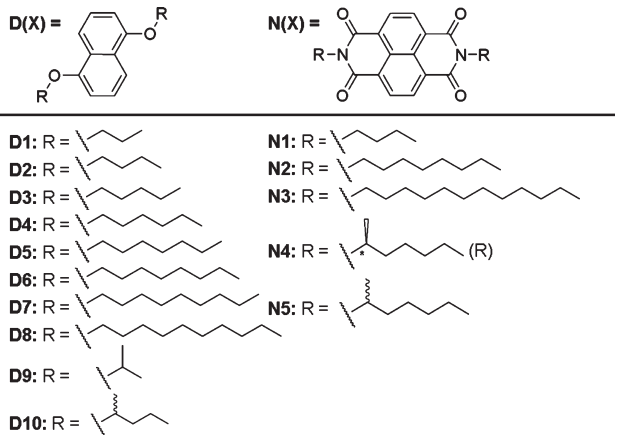

FIGURE 1. Dan and Ndi derivatives used in this study.

Results

Synthesis. Dan and Ndi derivatives were synthesized as described previously[6a] with slight modification[11] (Figure 1). Because our previous study revealed that the mesophase-crystallization phase transition temperature correlated with the Dan side chain identity, a series of Dan units with increasing alkyl chain lengths (D1−D8) were created to investigate systematically the effects of side chain length on the mesophase-crystalline phase transition behavior of the Dan:Ndi mixtures. Dan components with alkyl chains of one or two carbons evaporated readily during these experiments. Noting that the instantaneous color changes seemed characteristic of mixtures containing the diisopropyl Dan derivative in our previous study, we included branched alkyl chains (D9, D10) to study possible steric interactions. Ndi derivatives N1−N5 were selected as representative Ndi units possessing three different alkyl chain lengths as well as branching.

Characterization of Components. The individual components were analyzed by differential scanning calorimetry (DSC) to quantify transition temperatures as well as crystallization characteristics. DSC data for the components was collected on cooling after the second heating cycle at a rate of 5 °C/min. Component phase transition temperatures and associated enthalpies of crystallization are listed in Table 1. The crystallization temperatures of the linear components generally

(4) For examples, see: (a) Reczek, J. J.; Iverson, B. L. *Macromolecules* **2006**, *39* (17), 5601–5603. (b) Patrick, C. R.; Prosser, G. S. *Nature* (*London*) **1960**, 1021. (c) Koshkakaryan, G.; Klivansky, L. M.; Cao, D.; Snauko, M.; Teat, S. J.; Struppe, J. O.; Liu, Y. *J. Am. Chem. Soc.* **2009**, *131*, 2078–2079. (d) Hamilton, D. G.; Lynch, D. E.; Byriel, K. A.; Kennard, C. H. L. *Aust. J. Chem.* **1997**, *50*, 439–446. (e) Wang, C.; Yin, S.; Chen, S.; Xu, H.; Wang, Z.; Zhang, X. *Angew. Chem., Int. Ed.* **2008**, *47* (47), 9049–9052. (f) Jonkheijm, P.; Stutzmann, N.; Chen, Z.; de Leeuw, D. M.; Meijer, E. W.; Schenning, A. P. H. J.; Würthner, F. *J. Am. Chem. Soc.* **2006**, *128*, 9535.

(5) For examples, see: (a) Aprahamian, I.; Yasuda, T.; Ikeda, T.; Saha, S.; Dichtel, W. R.; Isoda, K.; Kato, T.; Stoddart, J. F. *Angew. Chem., Int. Ed.* **2007**, *46*, 4675–4679. (b) Percec, V.; Glodde, M.; Bera, T. K.; Miura, Y.; Shiyanovskaya, I.; Singer, K. D.; Balagurusamy, V. S. K.; Heiney, P. A.; Schnell, I.; Rapp, A.; Spiess, H.-W.; Hudson, S. D.; Duan, H. *Nature* **2002**, *419*, 384–387. (c) Pisula, W.; Kastler, M.; Wasserfallen, D.; Robertson, J. W. F.; Nolde, F.; Kohl, C.; Muellen, K. *Angew. Chem., Int. Ed.* **2006**, *45*, 819–823. (d) Lee, S. J.; Change, J. Y. *Tetrahedron Lett.* **2003**, *44*, 7493. (e) Arikainen, E.; O.; Boden, N.; Bushby, R. J.; Lozman, O. R.; Vinter, J. G.; Wood, A. *Angew. Chem., Int. Ed.* **2000**, *39*, 2333. (f) Weck, M.; Dunn, A. R.; Matsumoto, K.; Coates, G. W.; Lobkovsky, E. B.; Grubbs, R. H. *Angew. Chem., Int. Ed.* **1999**, *38*, 2741. (g) Praefcke, K.; Singer, D. In *Handbook of Liquid Crystals*; Demus, D., Goodby., J., Gary, G. W., Spiess, H. W., Vill, V., Eds.; Wiley-VCH: Weinheim, 1998; Vol. 2B, pp 945−967. (h) Bengs, H.; Ebert, M.; Karthaus, O.; Kohne, B.; Praefeke, K.; Ringsdorf, H.; Wendorff, J.; Wüstefeld, R. *Adv. Mater.* **1990**, *2*, 141. (i) Ringsdorf, H.; Wüstefeld, R.; Zerta, M.; Ebert, J.; Wendorff, J. *Angew. Chem.* **1989**, *101*, 934. (j) Goldmann, D.; Janietz, D.; Schmidt, C.; Wendorff, J. H. *Angew. Chem., Int. Ed.* **2000**, *39*, 1851. (k) Arikainen, E. O.; Boden, N.; Bushby, R. J.; Lozman, O. R.; Vinter, J. G.; Wood, A. *Angew. Chem., Int. Ed.* **2000**, *39*, 2333–2336. (l) Qu, S.; Chen, X.; Shao, X.; Li, F.; Zhang, H.; Wang, H.; Zhang, P.; Yu, Z.; Wu, K.; Wang, Y.; Li, M. *J. Mater. Chem.* **2008**, *18*, 3954–3964.

(6) (a) Reczek, J. J.; Villazor, K. R.; Lynch, V.; Swager, T. M.; Iverson, B. L. *J. Am. Chem. Soc.* **2006**, *128* (24), 7995. (b) Park, L. Y.; Hamiliton, D. G.; McGehee, E. A.; McMenimen, K. A. *J. Am. Chem. Soc.* **2003**, *125*, 10586.

(7) (a) O′Neill, M.; Kelly, S. M. *Adv. Mater.* **2003**, *15*, 1135. (b) van Breemen, A. J. J. M.; Herwig, P. T.; Chlon, C. H. T.; Sweelssen, J.; Schoo, H. F. M.; Setayesh, S.; Hardeman, W. M.; Martin, C. A.; de Leeuw, D. M.; Valeton, J. J. P.; Bastiaansen, C. W. M.; Broer, D. J.; Popa-Merticaru, A. R.; Meskers, S. C. J. *J. Am. Chem. Soc.* **2006**, *128*, 2336. (c) Simpson, C. D.; Wu, J.; Watson, M. D.; Muellen, K. *J. Mater. Chem.* **2004**, *14*, 494–504. (d) An, Z.; Yu, J.; Jones, S. C.; Barlow, S.; Yoo, S.; Domercq, B.; Prins, P.; Siebbeles, L. D. A.; Kippelen, B.; Marder, S. R. *Adv. Mater.* **2005**, *17*, 2580–2583. (e) Kato, T.; Mizoshita, N.; Kishimoto, K. *Angew. Chem., Int. Ed.* **2006**, *45*, 38–68. (f) Hoeben, F. J. M.; Jonkheijm, P.; Meijer, E. W.; Schenning, A. P. H. *J. Chem Rev.* **2005**, *105*, 1491–1546.

(8) (a) Leitch, A. A.; Reed, R. W.; Robertson, C. M.; Britten, J. F.; Yu, X.; Secco, R. A.; Oakley, R. T. *J. Am. Chem. Soc.* **2007**, *129*, 7903. (b) Shibahara, S.; Kitagawa, H.; Ozawa, Y.; Toriumi, K.; Kubo, T.; Nakasuji, K. *Inorg. Chem.* **2007**, *46*, 1162.

(9) (a) Okabe, A.; Fukushima, T.; Ariga, K.; Aida, T. *Angew. Chem., Int. Ed.* **2002**, *41*, 3414–3417. (b) Wang, J.-Y.; Yan, J.; Ding, L.; Ma, Y.; Pei, J. *Adv. Funct. Mater.* **2009**, *19*, 1746–1752.

(10) (a) Schmidt-Mende, L.; Fechtenkötter, A.; Müllen, K.; Moons, E.; Friend, R.; MacKenzie, J. *Science* **2001**, *293*, 1119–1122. (b) Sergeyev, S.; Pisula, W.; Geerts, Y. H. *Chem. Soc. Rev.* **2007**, *36*, 1902–1929.

(11) Pengo, P.; Pantos, G. D.; Otto, S.; Sanders, J. K. M. *J. Org. Chem.* **2006**, *71* (18), 7063.

TABLE 1. Component Crystallization Temperatures and Enthalpies[a]

derivative	T_c, °C (ΔH, kJ mol^{-1})
D1	97 (−20)
D2	95 (−25) → 78 (−24)
D3	70 (−44)
D4	81 (−61)
D5	64 (−47)
D6	76 (−71)
D7	59 (−39)
D8	81 (−87)
D9	98 (−36)
D10	24 (−22)
N1	226 (−23) → 160(−3)
N2	181 (−32)
N3	160 (−27) → 145 (−8)
N4	156 (−23)
N5	117 (−24)

[a]Temperatures (T_c) and associated enthalpies of crystallization (ΔH) obtained by DSC upon cooling at 5°C/min.

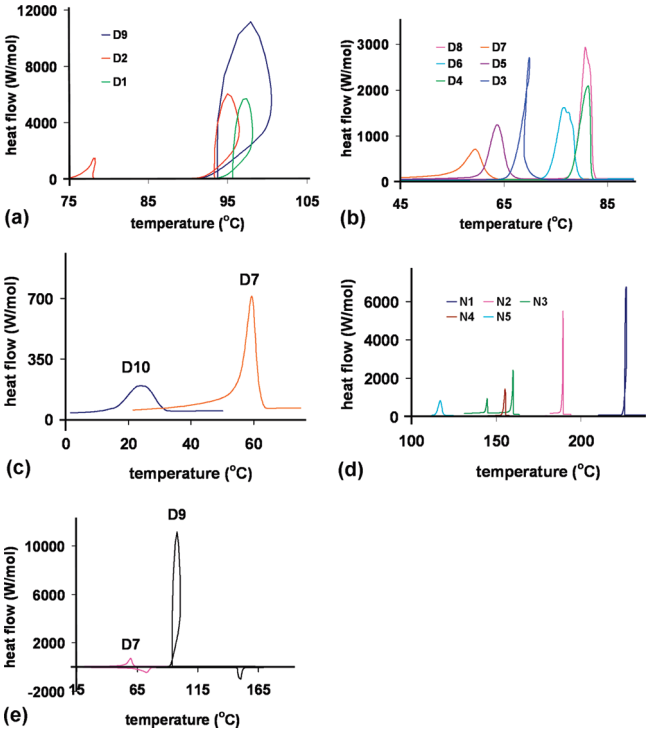

FIGURE 2. DSC traces upon cooling at 5 °C/min for all Dan and Ndi derivatives. (a) D1, D2, and D9 traces. (b) D3−D8 traces. (c) D10 with the D7 trace for comparison. (d) Ndi traces (N1's additional crystalline phase modification was omitted for clarity). (e) D9 heating and cooling cycles at 5 °C/min exhibited a significant supercooling effect, whereas D7 showed little supercooling.

decreased in an odd−even fashion (D1 > D3 > D5 > D7 and D2 > D4, D8 > D6), and higher magnitude transition enthalpies were usually observed with the longer alkyl chain derivatives.

The data in Figure 2a−c reveal that Dan units with alkyl substituents containing 4 or fewer carbons (D1, D2, and D9) resulted in crystallization heat flows (peak intensities) that were 2−3 times larger than those of the other Dan derivatives that had more broad exotherms. N1 and N2 also produced narrow, intense exotherms compared to the other Ndi components (Figure 2d). Branched or racemic alkyl chains resulted in lower crystallization points and broader transitions. The broad crystallization peaks of D10 and N5, Figure 2c,d, occurred at the lowest temperatures and were among the least energetic (in terms of ΔH) derivatives of this investigation. D2, N1, and N3 underwent two transitions, the origin of which is unclear at this time, but this behavior has previously been observed with long chain Ndi derivatives.[6a] Significant supercooling effects were observed for those derivatives with intense crystallization exotherms, particularly D1, D2, and D9 (Figure 2e).

X-ray Crystallography. Single crystal data were obtained for homocrystals of several Dan units to look for a correlation between crystal structure and the other properties examined in this study. In all cases, the Dan units packed in a herringbone (Figure 3c or f) or a completely offset planar fashion (Figure 3a,b and d,e). Structures of several Ndi derivatives were also determined and were found to stack in an offset face-to-face fashion as shown in Figure 3g−i. A cocrystal of D5:N4 (Figure 4) shows the aromatic donor−acceptor stacking mode that leads to the characteristic dark red color of these crystalline materials.

Mixtures. Mesophases were prepared by melting together 1:1 molar mixtures of solid Dan and Ndi derivatives in the absence of solvent. All 50 combinations of D1−D10 and N1−N5 were investigated. The lower melting point component (generally the Dan residue) melted first, thereby dissolving the higher melting point component. A liquid crystalline phase persisted until a completely isotropic mixture formed. As expected on the basis of our previous results,[6a] the mixture clearing temperature corresponded reasonably well with the crystallization temperature of the Ndi derivative and the mixture crystallization temperature corresponded reasonably well with the crystallization temperature of the Dan component upon cooling. In all cases, the liquid crystalline and isotropic phases exhibited a deep red color that is characteristic of the Dan-Ndi charge transfer (CT) band, indicating face-centered stacks with alternating Dan-Ndi units. Upon crystallization, the mixtures either remained dark red or lost their dark red color, indicating the preservation or loss of alternating Dan-Ndi stacks (Figure 5). Mixtures containing N5 did not appear to produce a liquid crystalline phase.

Representative examples of crystalline colors are shown in Figure 6. D1−D8:N4 and D1−D9:N5 retained a dark red (Figure 6a) color upon crystallization. Some mixtures such as D4−8:N2 appeared to exhibit a light pink crystalline color (Figure 6b), while all other mixtures completely lost their red intensity (Figure 6c) within a few minutes of cooling to the crystallization temperature.

A representative color change process is depicted in Figure 7 with a sample of D8:N1. The color change began in the center of the sample as it was located over the center of the heating stage (an area that cools first), then radiated outward with time until the entire sample was no longer red. This transition took about 20 s to complete. Importantly, the *macroscopic morphology, i.e., surface features, of the solid did not change during this process*, indicating reorganization at the microdomain level consistent with our previous observations.[6a]

UV−vis Spectroscopy. Thin crystalline films were examined using UV−vis spectroscopy to monitor the presence of the CT band by melting equimolar Dan:Ndi mixtures between two glass slides. Interestingly, placing the mixtures between the glass slides slowed the rate of color change upon crystallization compared to samples without a top cover.

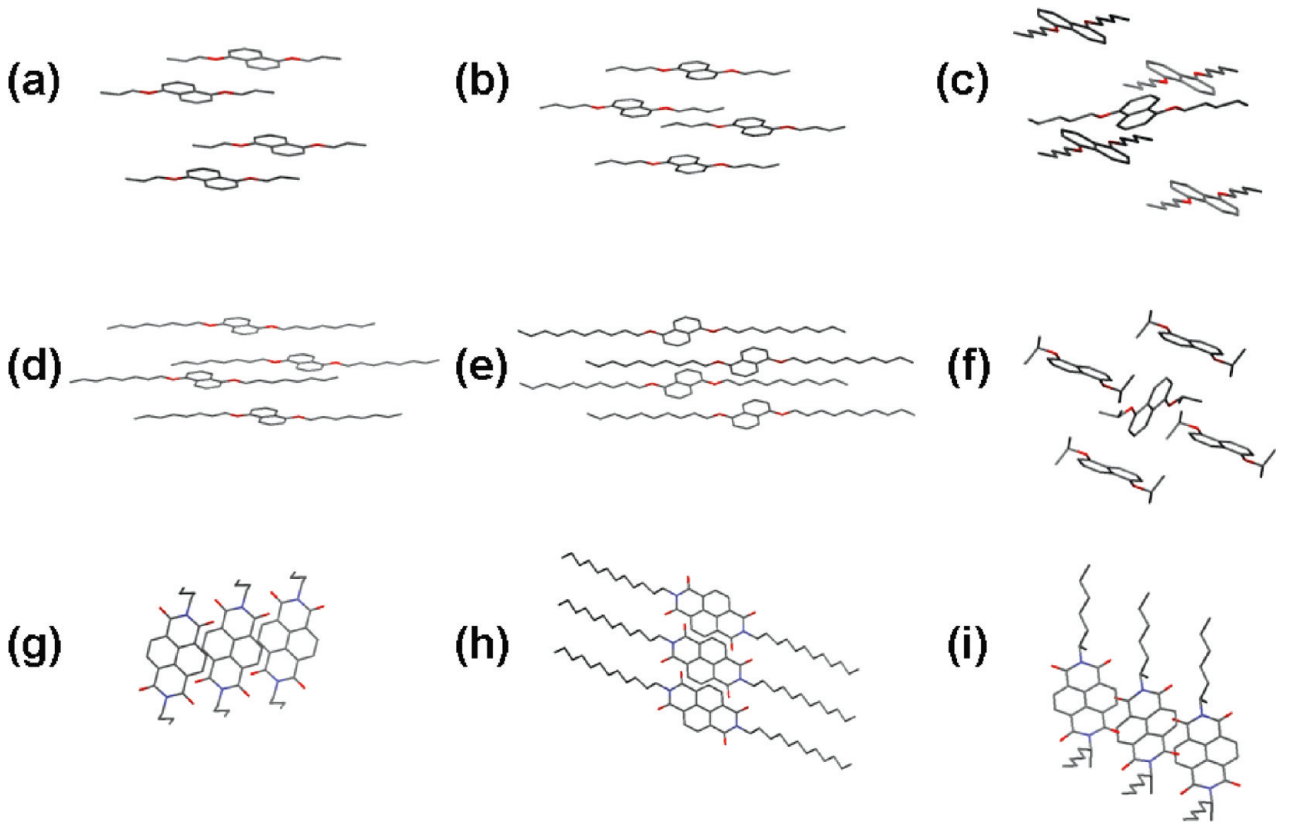

FIGURE 3. X-ray single-crystal structure of (a) D1, (b) D2, (c) D3, (d) D6, (e) D8, (f) D9, (g) N1, (h) N3, and (i) N4.

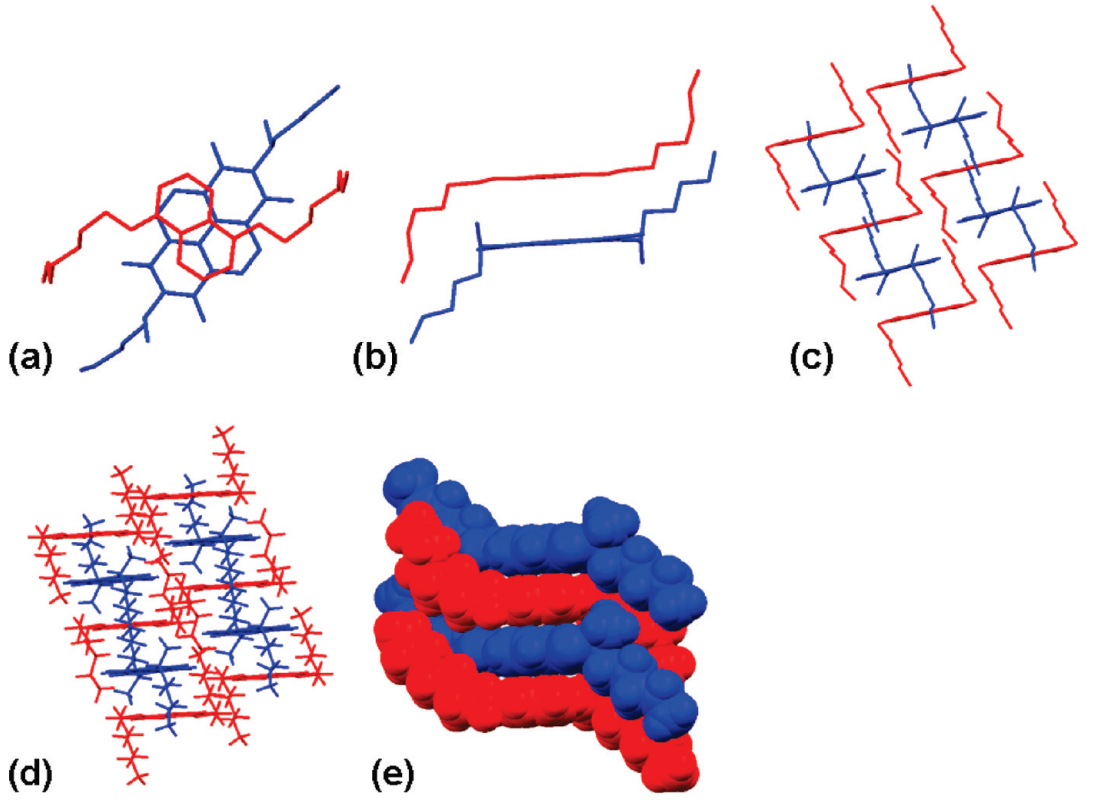

FIGURE 4. X-ray single-crystal structure of cocrystal D5:N4. Structures (a−c) are presented without hydrogen atoms for clarity. (d) Packing with the hydrogen atoms. (e) Space-filled structures with hydrogen atoms.

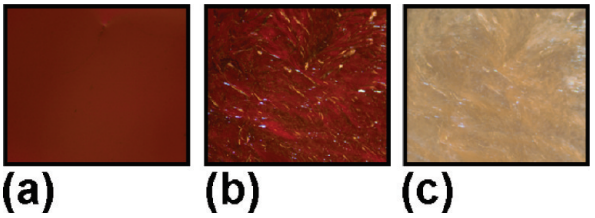

FIGURE 5. Thermochromic behavior taken under 5X magnification for D8:N3 on cooling: (a) 145, (b) 110, and (c) 60 °C.

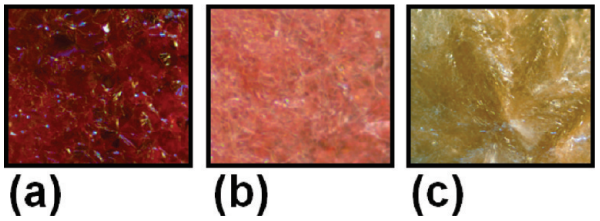

FIGURE 6. Representative colors for bulk crystalline phases taken under 5X magnification: (a) D9:N5, (b) D4:N2, and (c) D7:N3.

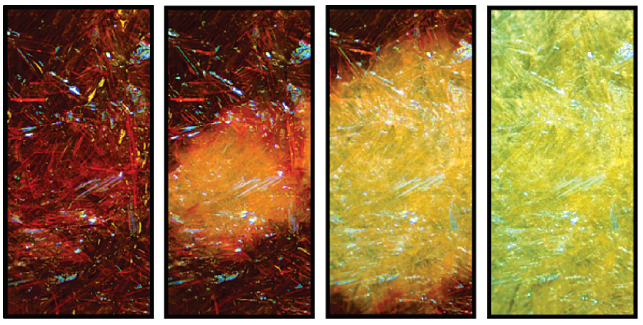

FIGURE 7. Deep red mesophase to off-white crystalline phase color change (5X magnification) that occurred over approximately 20 s of cooling for the D8:N1 mixture.

Therefore, in order to ensure completion of the phase transition, UV−vis spectra were collected after the mixtures cooled for at least 5 min following attainment of the crystallization temperature.[6a] Mixtures containing D10 had to be placed at 20 °C for 10 min to ensure complete crystallization. Representative UV−vis spectra are shown in Figure 8. The thermochromic behavior was recorded as the retention or loss of the CT absorbance (Table 2). Those mixtures that maintained a deep red color upon crystallization (most mixtures with N4 and N5) exhibited the expected strong CT absorbance in their crystalline state (Figure 8a). Mixtures that changed color from deep red to pink (D4−D8:N2) displayed a CT absorbance dramatically reduced in intensity and red-shifted (Figure 9). The CT absorbance of the pink samples can be better visualized upon subtraction of the D9:N2 spectrum, which cancels some of the background scattering (Figure 10). The extremely small, red-shifted absorption profile is consistent with a crystalline state in which an incomplete separation of the alternating donor−acceptor molecules has taken place, leading to the faint pink color.

Differential Scanning Calorimetry. The phase transitions of the mixtures were characterized using DSC. Phase transition temperatures and energies measured at a cooling rate of 2 °C/min for the mixtures of D1−10 with N1−N5 are given in Tables 3−7. All mixtures measured, except those that contained N5, produced at least two transition temperatures that indicated mesophase formation. D10:N5 was extremely slow to crystallize, and transition temperatures were not obtained for this mixture by DSC.

Polarized Optical Microscopy. Mesophase texture visualization and transition temperature confirmation were performed using polarized optical microscopy (POM). Samples were placed between glass coverslips and analyzed upon cooling from the isotropic phase at a rate of 5 °C/min. Textures (Figure 11) were consistent with those previously reported for Dan:Ndi mixtures.[6a] The long sheet-like dendritic or mosaic patterns are characteristic of columnar mesophases.[13]

Discussion

Individual Component Crystallization Behavior. The DSC traces of D1−D10 (Table 1 and Figure 2) revealed that several Dan derivatives (D1, D2, and D9) exhibited looping patterns upon crystallization. The peak intensities for these derivatives were among the largest seen in this study and their observed crystallization temperatures were several degrees lower than their melting temperatures. In other words, these samples behaved as supercooled liquids during the cooling cycle. Once nucleation occurred, crystals grew rapidly, leading to self-heating that was manifest in the observed looping traces.[14] Taken together, the relatively large heat flows and higher crystallization temperatures indicated that D1, D2, and D9 produced a highly crystalline material with a rapid growth process once nucleation had begun. Of the Ndi derivatives examined, N1 and N2 had relatively large heat flows and showed some self-heating behavior, indicating that these also formed highly crystalline materials upon nucleation.

Those components with longer side chains such as D3−D8 and N3 resulted in more gradual exotherms at lower temperatures that were less intense and exhibited negligible supercooling behavior. Presumably, the longer side chains slowed down the organization process during crystallization. With the exception of the short-chain D9 derivative, branching (D10, N4−5) lowered the exotherm intensity and crystallization temperature significantly. The racemic nature of the D10 and N5 (as compared to enantiomerically pure N4) analogues also complicated the crystallization process as they had the lowest crystallization temperatures and the least intense exotherms of any derivatives examined.

We initially sought to determine if there was a correlation between an individual component's crystallization behavior and the presence or absence of significant color change of the 1:1 mixtures made from it. Overall, derivatives with relatively intense exothermic transitions such as D1−D3 and N3 also exhibited the highest melting temperatures, an indication that these derivatives make particularly stable homocrystals. Such stability would provide a possible thermodynamic driving force for phase separation during the mesophase to

(12) A few enthalpy values in our previous report appear too large by an order of magnitude (particularly those for the Dan components). Enthalpy values have been obtained from transition exotherm integrations performed by the TA Universal Analysis program. Any discrepancy regarding transition temperatures may be the result of different scan rates and or supercooling effects.

(13) Dierking, I. *Textures of Liquid Crystals*; Wiley-VCH: Weinheim, 2003; pp 147−148, 165, 207−208.

(14) (a) TA Instruments. Aubuchon, S. R. *Interpretation of the Crystallization Peak of Supercooled Liquids Using Tzero® DSC*. http://www.tainstruments.com (b) Danley, R. L. *Thermochim. Acta* **2004**, *409*, 111–119.

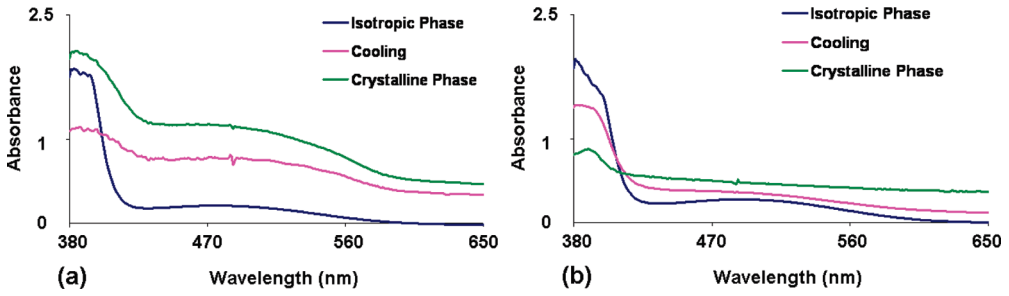

FIGURE 8. Representative UV−vis spectra on cooling for (a) D7:N4 (retention of CT) and (b) D7:N3 (loss of CT).

TABLE 2. Crystalline Final Color of Mixtures[a]

	N1	N2	N3	N4	N5
D1	–	L	L	R	R
D2	–	L	L	R	R
D3	–	L	L	R	R
D4	–	P	L	R	R
D5	L	P	L	R	R
D6	L	P	L	R	R
D7	L	P	L	R	R
D8	L	P	L	R	R
D9	–	L	L	L	R
D10	–	L	L	L	L

[a]The thermochromic behavior is reported as the retention (R), change to pink (P), or loss (L) with respect to the observed deep red color of the mesophase upon crystallization. Dashes indicate component evaporation.

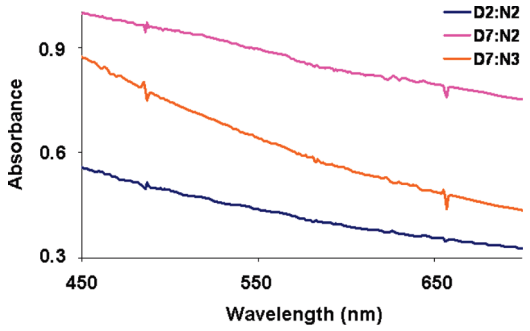

FIGURE 9. Expanded CT region and slight absorption for crystalline D7:N2 (pink). D2:N2 (loss of red color) and D7:N3 (loss of red color) are shown for comparison.

crystal transition of mixtures. However, high melting temperature is not the only important parameter for unstacking during mixture crystallization as all derivatives with linear side chains produced mixtures that unstacked, regardless of the individual component crystallization properties.

Individual Component Structure. Structures of several representative Dan and Ndi units were obtained to compare crystalline structures to measured properties such as the DSC traces. In all of the Dan X-ray structures, the aromatic core units stacked in a planar offset or herringbone manner, never in an arrangement involving any parallel aromatic stacking. On the other hand, all Ndi structures obtained in this study contained an offset face-to-face aromatic stacking mode. For the Dan component structures obtained, no obvious correlation between the modes of aromatic stacking, i.e., herringbone versus planar offset, and the DSC traces of the Dan components was seen. For example, D1 and D3 exhibited very similar DSC traces with moderate heat flow and some looping behavior, but D1 crystallized in a planar offset mode, while D3 crystallized in a herringbone arrangement (Figure 3). Similarly, although individual Ndi derivatives exhibited different DSC traces, all of their crystals showed similar packing. To a first approximation, then, it appears appropriate to attribute the DSC behavior to side chain packing interactions rather than the aromatic stacking mode of the Dan or Ndi derivatives.

Mesophase Behavior of Mixtures. DSC studies of most mixtures exhibited at least two transitions, consistent with mesophase formation (Tables 3−7). Optical textures obtained through POM supported the formation of columnar mesophases (Figure 11). The only mixtures that did not appear to form a true mesophase were those with N5, possibly a manifestation of its racemic nature. The DSC data for the various mixtures was consistent with the previously reported trend that major transition temperatures correlated in a *relative way* to the transition temperatures of the components. For example, D4:N2 crystallized at 78 °C (D4 = 81 °C) and D6:N2 crystallized at 76 °C (D6 = 76 °C). Clearing point temperatures occurred around 180 °C with N1 (N1 = 226 °C), 140 °C with N2 (N2 = 181 °C), and 130 °C with N3 (N3 = 160 °C). A likely explanation for these correlations is that the Dan and Ndi side chains are positioned orthogonal to each other in the face-centered Dan-Ndi stack, so they behave independently of each other, consistent with their behavior in pure form. This observation is consistent with our previous report[6a] as well as the X-ray crystallography results reported here and supports the hypothesis that side chain interactions dominate phase transition behavior.

Thermochromic Behavior of Mixtures. The present study was intended to investigate the thermochromic behavior of Dan:Ndi mixtures in a systematic fashion. Here, only D1−8:N4 and D1−9:N5 remained dark red upon crystallization, while all other mixtures examined lost their red mesophase color. There are at least two explanations for the observed thermochromic behavior. In one scenario, separation into Dan and Ndi microdomains occurs during the crystallization process.[6a] Alternatively, the aromatic units could rearrange to give an overall altered but homogeneous packing in which the alternating aromatic stacking is diminished, such as in a herringbone arrangement or some other offset packing. Our previous results using X-ray powder diffraction studies verified that in the case of D9:N4 the observed thermochromism was the result of separation into Dan and Ndi microdomains upon crystallization.[6a] Unexpectedly, several crystalline mixtures, especially those involving N2, exhibited a light pink color (Figure 6 and Table 2). The light pink color of these mixtures (for example D7:N2) could result from incomplete

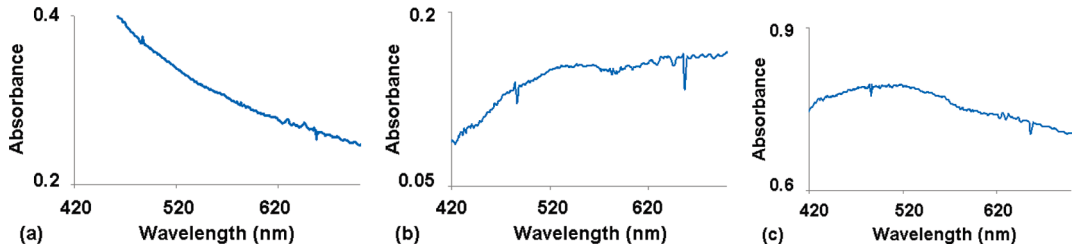

FIGURE 10. UV−vis spectra of the CT region for representative mixtures in the N2 series with D9:N2 subtraction correction: (a) D9:N2, no CT band; (b) D8:N2, slight CT absorption; (c) D7:N2, slight CT absorption.

TABLE 3. Thermal Phase Behavior Characterization of 1:1 Mixtures of D1−10:N1[a]

derivative		T_{c1}	→	T_{c2}	→	T_{c3}	
D1:N1				D1 evaporated			
D2:N1				D2 evaporated			
D3:N1				D3 evaporated			
D4:N1				D4 evaporated			
D5:N1	iso	188 [−13]	→	72 [−31]	→	55 [−87]	cr
D6:N1	iso	182 [−4]	→	71[b] [−82]			cr
D7:N1	iso	176 [−13]	→	71 [−19]	→	53 [−43]	cr
D8:N1	iso	182 [−8]	→	74[b] [−93]			cr
D9:N1				D9 evaporated			
D10:N1				D10 evaporated			

[a]Temperatures (°C) and enthalpies (KJ/mol) in brackets for phase transitions determined by DSC upon cooling 2°C/min. T_c is a transition upon cooling; iso = isotropic and cr = final crystalline state. [b]Transition is composed of multiple peaks.

TABLE 4. Thermal Phase Behavior Characterization of 1:1 Mixtures of D1−10:N2[a]

derivative		T_{c1}	→	T_{c2}	→	T_{c3}	
D1:N2				D1 evaporated			
D2:N2	iso	137 [−10]	→	86 [−28]	→	81[b] [−22]	cr
D3:N2	iso	139 [−8]	→	64 [−47]			cr
D4:N2	iso	148 [−7]	→	78 [−63]			cr
D5:N2	iso	138 [−9]	→	60 [−55]			cr
D6:N2	iso	140 [−8]	→	76 [−74]			cr
D7:N2	iso	146 [−7]	→	68 [−68]			cr
D8:N2	iso	141 [−6]	→	78 [−92]			cr
D9:N2				D9 evaporated			
D10:N2	iso	144 [−10]	→	41 [−0.6]			cr

[a]Temperatures (°C) and enthalpies (KJ/mol) in brackets for phase transitions determined by DSC upon cooling 2°C/min. T_c is a transition upon cooling; iso = isotropic and cr = final crystalline state. [b]Transition is composed of multiple peaks.

TABLE 5. Thermal Phase Behavior Characterization of 1:1 Mixtures of D1−10:N3[a]

derivative		T_{c1}	→	T_{c2}	→	T_{c3}	
D1:N3	iso	132 [−7]	→	86 [−22]			cr
D2:N3	iso	134 [−7]	→	85 [−25]	→	73 [−15]	cr
D3:N3	iso	129 [−11]	→	66 [−46]			cr
D4:N3	iso	131 [−10]	→	77 [−67]			cr
D5:N3	iso	123 [−21]	→	60 [−49]			cr
D6:N3	iso	123 [−21]	→	75 [−72]			cr
D7:N3	iso	129 [−14]	→	66 [−71]			cr
D8:N3	iso	133 [−17]	→	78 [−85]			cr
D9:N3	iso	125 [−7][b]	→	132[b] [−38]			cr
D10:N3	iso	131 [−17]	→	120 [−0.4]			cr

[a]Temperatures (°C) and enthalpies (KJ/mol) in brackets for phase transitions determined by DSC upon cooling 2°C/min. T_c is a transition upon cooling; iso = isotropic and cr = final crystalline state. [b]Transition is composed of multiple peaks.

TABLE 6. [12] **Thermal Phase Behavior Characterization of 1:1 Mixtures of D1−10:N4**[a]

derivative		T_{c1}	→	T_{c2}	→	T_{c3}	
D1:N4				D1 evaporated			
D2:N4	iso	116 [−4]	→	103 [−17]	→	83 [−9]	cr
D3:N4	iso	121 [−7]	→	99 [−18]	→	65 [−22]	cr
D4:N4	iso	129 [−5]	→	122 [−41]	→	72 [−5]	cr
D5:N4	iso	133 [−11]	→	124 [−35]			cr
D6:N4	iso	123[b] [−5]	→	121[b] [−40]			cr
D7:N4	iso	124 [−7]	→	112 [−35]			cr
D8:N4	iso	115 [−7]	→	99 [−20]	→	61 [−18]	cr
D9:N4	iso	115 [−10]	→	80 [−42]	→	76 [−49]	cr
D10:N4	iso	122 [−11]	→	20 [−15]			cr

[a]Temperatures (°C) and enthalpies (KJ/mol) in brackets for phase transitions determined by DSC upon cooling 2°C/min. T_c is a transition upon cooling. iso = isotropic and cr = final crystalline state. [b]Transition is composed of multiple peaks.

TABLE 7. Thermal Phase Behavior Characterization of 1:1 Mixtures of D1−10:N5[a]

derivative		T_{c1}	→	T_{c2}	→	T_{c3}	
D1N5	iso	95 [−0.7]	→	84 [−5]			cr
D2N5	iso	98 [−42]	→	89 [−3]	→	63 [−1]	cr
D3N5	iso	95 [−37]	→	61 [−10]			cr
D4N5	iso	111 [−52]	→	77 [−3]			cr
D5N5	iso	110 [−54]	→	50 [−11]			cr
D6N5	iso	110 [−59]	→	73 [−3]			cr
D7N5	iso	106 [−58]	→	55 [−3]			cr
D8N5	iso	94 [−55]	→	74 [−16]			cr
D9N5	iso	106 [−50]	→	81 [−3]			cr
D10N5	iso	–		–			

[a]Temperatures (°C) and enthalpies (KJ/mol) in brackets for phase transitions determined by DSC upon cooling 2°C/min. T_c is a transition upon cooling; iso = isotropic and cr = final crystalline state. Dashes indicate no observed exothermic transitions.

separation into microdomains or, in the second scenario, a novel packing mode with a modified or diminished CT absorbance (Figure 9 and Figure 10).

It is worth noting that the color change associated with mixtures containing D9 occurred more rapidly than with the other Dan derivatives with linear side chains, happening almost instantaneously versus a few seconds for the straight-chain derivatives. The rapid color change associated with D9 in this study is consistent with our previous observations.[6a] A reasonable explanation for this behavior is that the steric strain resulting from the isopropyl side chain of D9 in close proximity to the Ndi aromatic core increases the rate of component separation during crystallization.

Cocrystal Structure. The crystallographic structure obtained for the deep red D5:N4 mixture showed face-centered stacks of alternating Dan:Ndi units (Figure 4a−e). The component side chains are positioned in an orthogonal fashion as expected.[6a] The branched Ndi side chains are oriented above and below the Ndi plane and, importantly,

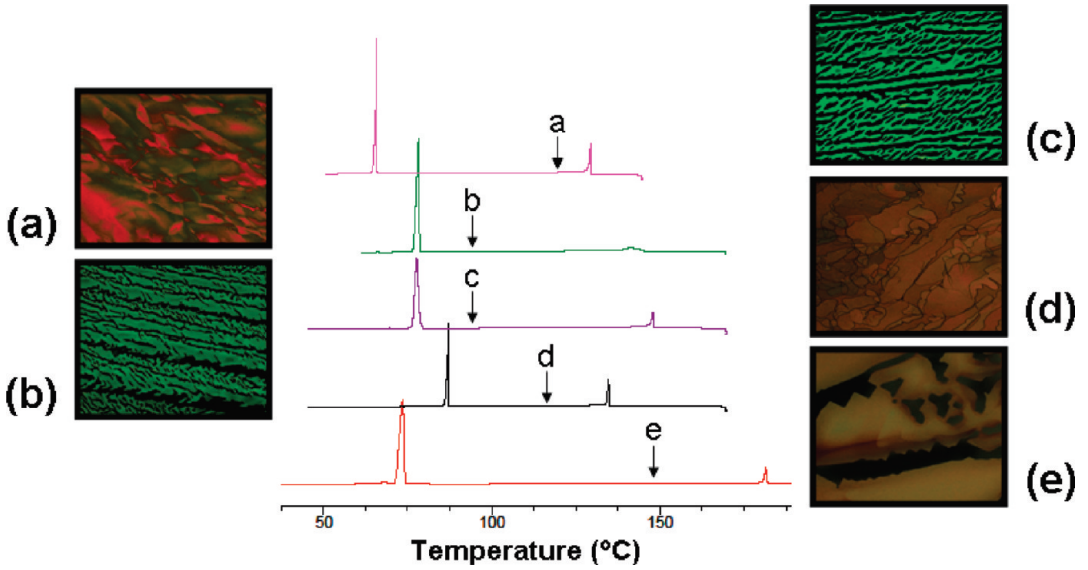

FIGURE 11. Optical textures and associated DSC traces for representative 1:1 mixtures at 10X magnification. Arrows indicate optical texture temperatures: (a) D3:N3, 118 °C; (b) D8:N2, 92 °C; (c) D4:N2, 90 °C; (d) D1:N2, 117 °C; (e) D8:N1, 147 °C.

appear to surround the Dan units while in the alternating stacks (Figure 4d,e). Close inspection reveals that indeed the N4 branch methyl group is likely to serve as a steric barrier to unstacking, perhaps "locking in" the alternating aromatic stack enough for it to persist in the crystalline state.

Conclusions

A more complete understanding of intermolecular Dan-Ndi interactions in different phases has emerged from the present work. In particular, complementary electrostatic interactions between the aromatic cores apparently dominate the Dan-Ndi packing arrangement when some or all of the side chains are mobile, verified by the characteristic red color due to alternating face-to-face stacking in the isotropic and mesophases with all mixtures. During crystallization, however, the interactions of the side chains appear to become dominant, often leading to dramatic thermochromism as unstacking of the aromatic cores leads to loss of the CT absorption and corresponding red color.

A lack of thermochromic behavior during the mesophase to crystalline phase transition was seen with mixtures containing N4 and N5. The D5:N4 cocrystal (Figure 4) revealed that the methyl group of the branched side chain on N4 virtually encloses D5 within the stack, apparently preventing unstacking during crystallization. Interestingly, the D9−10:N4 mixtures did undergo a color change, indicating that Dan side chain branching can serve as a stacking deterrent even in the presence of such a presumed Ndi rearrangement barrier.

The present study has shown that careful selection of Dan and Ndi components not only permits a high degree of mesophase tunability but also *controllable thermochromism*. For example, the change from a deep red mesophase to a deep red or an off-white solid could be adjusted by changing branching on the Ndi side chain while maintaining the same Dan component. Future work will aim to refine these relationships; in particular the stereochemical affects of the components as well as develop Dan and Ndi mixtures exhibiting robust mesophase behavior at or around room temperature.

Experimental Section

General Methods. All compounds were synthesized in a 60−80% yield using modifications of previously reported methods.[6,11] A CEM Microwave Accelerated Reaction System (model MARS) was used to synthesize the Ndi derivatives.

Generic Dan Preparation. To a solution of 1,5-dihydroxynaphthalene (1 equiv) and K_2CO_3 (5 equiv) in CH_3CN (0.1 M) was added 1-bromo-alkane (2.4 equiv). The solution was heated to reflux and allowed to stir for 24 h. The solution was filtered while hot and concentrated under reduced pressure. The crude product was purified twice by column chromatography (20% CH_2Cl_2/80% hexanes) to afford the symmetrical Dan derivative. Suitable crystals for X-ray crystallographic analysis were obtained through slow evaporation from CH_2Cl_2.

Generic Ndi Preparation. A DMF (0.1 M) solution consisting of 1,4,5,8-naphthalenetetracarboxylic dianhydride (1 equiv), TEA (2.4 equiv), and 1-amino-alkane (2.4 equiv) was placed in a microwave reactor at 600 W. The temperature was ramped for 2 min until it reached 140 °C and was held at that temperature for 12 min. Once cooled, the solution was placed in a refrigerator for several hours. The precipitated product was removed by vacuum filtration. The crude product was purified by column chromatography (70% CH_2Cl_2/30% hexanes) to afford the symmetrical Ndi derivative. Suitable crystals for X-ray crystallographic analysis were obtained through slow evaporation from CH_2Cl_2.

Cocrystal Structure. Suitable crystals for X-ray crystallographic analysis of D5:N4 were obtained by slow evaporation of a 1:1 molar mixture of D5 and N4 from toluene.

1,5-Bis(propyloxy)naphthalene (D1). Mp 113−117 °C; ^{13}C NMR (400 MHz, $CDCl_3$) δ 154.3, 126.5, 124.7, 113.7, 105.0, 69.3, 22.4, 10.5 ppm; ^{1}H NMR (400 MHz, $CDCl_3$) δ 7.86 (d, J = 8.4 Hz, 2H), 7.35 (t, J = 7.6 Hz, 2H), 6.84 (d, J = 7.6, 2H), 4.09 (t, J = 6.4 Hz, 4H), 1.94 (m, 4H) 1.13 (t, J = 7.6 Hz, 6H) ppm; CI-HRMS (positive ion) calculated for $C_{16}H_{20}O_2$, 244.1463, found 244.1462.

1,5-Bis(butyloxy)naphthalene (D2). Mp 110−112 °C; ^{13}C NMR (400 MHz, $CDCl_3$) δ 154.7, 126.8, 125.0, 114.0, 105.2, 67.8, 31.4, 19.5, 14.0 ppm; ^{1}H NMR (400 MHz, $CDCl_3$) δ 7.86 (d, J = 8.8 Hz, 2H), 7.36 (t, J = 7.6 Hz, 2H), 6.83 (d, J = 7.6, 2H), 4.14 (t, J = 6.4 Hz, 4H), 1.91 (m, 4H), 1.61 (m, 4H), 1.03 (t, J = 7.2 Hz, 6H) ppm; CI-HRMS (positive ion) calculated for $C_{18}H_{24}O_2$, 272.1776, found 272.1773.

1,5-Bis(pentyloxy)naphthalene (D3). Mp 82−87 °C; ^{13}C NMR (400 MHz, $CDCl_3$) δ 154.56, 126.7, 124.9, 113.9, 105.1, 68.0, 28.9, 28.3, 22.4, 14.0 ppm; ^{1}H NMR (400 MHz, $CDCl_3$) δ 7.87 (d, J = 8.4 Hz, 2H), 7.36 (t, J = 7.6 Hz, 2H), 6.84 (d, J = 7.6 Hz, 2H), 4.13 (t, J = 6.4 Hz, 4H), 1.94 (m, 4H), 1.56 (m, 4H), 1.46 (m, 4H), 0.98 (t, J = 7.2 Hz, 6H) ppm; CI-HRMS (positive ion) calculated for $C_{20}H_{28}O_2$, 300.2089, found 300.2090.

1,5-Bis(hexyloxy)naphthalene (D4). Mp 90−93 °C; ^{13}C NMR (400 MHz, $CDCl_3$) δ 154.9, 126.8, 125.0, 114.0, 105.2, 68.2, 31.9, 29.33, 26.29, 22.7, 14.1 ppm; ^{1}H NMR (400 MHz, $CDCl_3$) δ 7.85 (d, J = 8.4 Hz, 2H), 7.35 (t, J = 7.6 Hz, 2H), 6.83 (d, J = 7.6 Hz, 2H), 4.12 (t, J = 6.4 Hz, 4H), 1.92 (m, 4H), 1.57 (m, 4H), 1.39 (m, 8H), 0.93 (t, J = 6.4 Hz, 6H) ppm; CI-HRMS (positive ion) calculated for $C_{22}H_{32}O_2$, 328.2402, found 328.2405.

1,5-Bis(heptyloxy)naphthalene (D5). Mp 72−82 °C; ^{13}C NMR (400 MHz, $CDCl_3$) δ 154.8, 126.8, 125.0, 114.0, 105.2, 68.2, 31.8, 29.3, 29.1, 26.3, 22.6, 14.1 ppm; ^{1}H NMR (400 MHz, $CDCl_3$) δ 7.85 (d, J = 8.4 Hz, 2H), 7.35 (t, J = 7.6 Hz, 2H), 6.82 (d, J = 7.6 Hz, 2H), 4.11 (t, J = 6.8 Hz, 4H), 1.92 (m, 4H), 1.56 (m, 4H), 1.34 (m, 12H), 0.91 (t, J = 6.8 Hz, 6H) ppm; CI-HRMS (positive ion) calculated for $C_{24}H_{36}O_2$, 356.2715, found 356.2715.

1,5-Bis(octyloxy)naphthalene (D6). Mp 86−94 °C; ^{13}C NMR (400 MHz, $CDCl_3$) δ 154.5, 126.6, 124.8, 113.9, 105.1, 68.0, 31.7, 29.25, 29.17, 29.12, 26.1, 22.5, 14.0 ppm; ^{1}H NMR (400 MHz, $CDCl_3$) δ 7.86 (d, J = 8.8 Hz, 2H), 7.35 (t, J = 7.6 Hz, 2H), 6.83 (d, J = 7.6 Hz, 2H), 4.12 (t, J = 6.4 Hz, 4H), 1.92 (m, 4H), 1.57 (m, 4H), 1.32 (m, 16H), 0.91 (t, J = 6.8 Hz, 6H) ppm; CI-HRMS (positive ion) calculated for $C_{26}H_{40}O_2$, 384.3028, found 384.3030.

1,5-Bis(nonyloxy)naphthalene (D7). Mp 75−84 °C; ^{13}C NMR (400 MHz, $CDCl_3$) δ 154.7, 126.8, 125.0, 114.0, 105.2, 68.2, 31.9, 29.57, 29.45, 29.33, 29.29, 26.3, 22.7, 14.1 ppm; ^{1}H NMR (400 MHz, $CDCl_3$) δ 7.85 (d, J = 8.4 Hz, 2H), 7.36 (t, J = 8.0 Hz, 2H), 6.83 (d, J = 7.6 Hz, 2H), 4.12 (t, J = 6.8 Hz, 4H), 1.92 (m, 4H), 1.57 (m, 4H), 1.30 (m, 20H), 0.90 (t, J = 6.8 Hz, 6H) ppm; CI-HRMS (positive ion) calculated for $C_{28}H_{44}O_2$, 412.3341, found 412.3341.

1,5-Bis(decyloxy)naphthalene (D8). Mp 94−97 °C; ^{13}C NMR (400 MHz, $CDCl_3$) δ 154.7, 126.8, 125.0, 114.0, 105.2, 68.2, 31.9, 29.6, 29.6, 29.4, 29.3, 26.3, 22.7, 14.1 ppm; ^{1}H NMR (400 MHz, $CDCl_3$) δ 7.84 (d, J = 8.4 Hz, 2H), 7.34 (t, J = 8.0 Hz, 2H), 6.82 (d, J = 7.6 Hz, 2H), 4.12 (t, J = 6.4 Hz, 4H), 1.92 (m, 4H), 1.54 (m, 4H), 1.28 (m, 24H), 0.89 (t, J = 7.2 Hz, 6H) ppm; CI-HRMS (positive ion) calculated for $C_{30}H_{48}O_2$, 440.3654, found 440.3655.

1,5-Bis(isopropoxy)naphthalene (D9). Mp 147−153 °C; ^{13}C NMR (400 MHz, $CDCl_3$) δ 153.7, 128.2, 125.2, 114.7, 107.4, 70.6, 22.4 ppm; ^{1}H NMR (400 MHz, $CDCl_3$) δ 7.89 (d, J = 8.1 Hz, 2H), 7.40 (t, J = 7.5 Hz, 2H), 6.90 (d, J = 7.5 Hz, 2H), 4.76 (m, 2H), 1.49 (d, J = 6 Hz, 12H) ppm; ESI-MS (positive ion, M + H^+) calculated for $C_{16}H_{20}O_2$ + H, 245, found 245.[1]

1,5-Bis(pentan-2-yloxy)naphthalene (D10). Mp 47−70 °C; ^{13}C NMR (400 MHz, $CDCl_3$) δ 153.7, 127.8, 124.9, 114.1, 106.6, 73.8, 38.8, 19.7, 18.8, 14.1 ppm; ^{1}H NMR (400 MHz, $CDCl_3$) δ 7.84 (d, J = 8.8 Hz, 2H), 7.34 (t, J = 8.0 Hz, 2H), 6.85 (d, J = 7.2 Hz, 2H), 4.58 (m, 2H), 1.88 (m, 2H), 1.68 (m, 2H), 1.55 (m, 4H), 1.40 (d, J = 6.0 Hz, 6H) 0.97 (t, J = 7.6 Hz, 6H) ppm; CI-HRMS (positive ion) calculated for $C_{20}H_{28}O_2$, 300.2089, found 300.2086.

2,7-Dibutyl-benzo[*lmn*][3,8]phenanthroline-1,3,6,8-tetraone (N1). Mp 232−239 °C; ^{13}C NMR (400 MHz, $CDCl_3$) δ 162.7, 130.8, 126.6, 126.5, 40.7, 30.1, 20.9, 13.8 ppm; ^{1}H NMR (400 MHz, $CDCl_3$) δ 8.71 (s, 4H), 4.17 (t, J = 7.6 Hz, 4H), 1.71 (m, 4H), 1.44 (m, 4H), 0.97 (t, J = 7.2 Hz, 6H) ppm; CI-HRMS (positive ion, M + H^+) calculated for $C_{22}H_{22}N_2O_4$ + H, 379.1613, found 379.1660.

2,7-Dioctyl-benzo[*lmn*][3,8]phenanthroline-1,3,6,8-tetraone (N2). Mp 184−187 °C; ^{13}C NMR (400 MHz, $CDCl_3$) δ 162.8, 130.9, 126.6, 126.6, 41.0, 31.8, 29.27, 29.17, 28.0, 27.1, 22.6, 14.1 ppm; ^{1}H NMR (400 MHz, $CDCl_3$) δ 8.74 (s, 4H), 4.18 (t, J = 8.0 Hz, 4H), 1.73 (m, 4H), 1.36 (m, 20H), 0.87 (t, J = 6.4 Hz, 6H) ppm; CI-HRMS (positive ion, M + H^+) calculated for $C_{30}H_{38}N_2O_4$+ H, 491.2910, found 491.2906.

2,7-Didodecyl-benzo[*lmn*][3,8]phenanthroline-1,3,6,8-tetraone (N3). Mp 161−163 °C; ^{13}C NMR (400 MHz, $CDCl_3$) δ 162.8, 130.9, 126.6, 126.6, 41.0, 31.9, 29.61, 29.58, 29.51, 29.40, 29.33 (one overlapping peak), 28.1, 27.1, 22.7, 14.1 ppm; ^{1}H NMR (400 MHz, $CDCl_3$) δ 8.74 (s, 4H), 4.18 (t, J = 7.6 Hz, 4H), 1.73 (m, 4H), 1.24 (m, 36H), 0.87 (t, J = 6.8 Hz, 6H) ppm; CI-HRMS (positive ion, M + H^+) calculated for $C_{38}H_{54}N_2O_4$ + H, 603.4162, found 603.4158.

2,7-Di(*R*-heptan-2-yl)benzo[*lmn*][3,8]phenanthroline-1,3,6,8-tetraone (N4). Mp 166−177 °C; $[\alpha]^{24}_D$+82.2 (*c* 0.6 CH_2Cl_2); ^{13}C NMR (400 MHz, $CDCl_3$) δ 163.6, 141.1, 131.1, 127.0, 50.7, 33.6, 31.8, 26.9, 22.8, 18.5, 14.2 ppm; ^{1}H NMR (400 MHz, $CDCl_3$) δ 8.74 (s, 4H), 5.28 (m, 2H), 2.19 (m, 2H), 1.91 (m, 2H), 1.61 (d, J = 7.2 Hz, 6H), 1.30 (m, 12H), 0.85 (t, J = 7.5 Hz, 6H) ppm; ESI-MS (positive ion, M + H^+) calculated for $C_{28}H_{34}N_2O_4$+ H, 463, found 463.[1]

2,7-Diheptan-2-yl-benzo[*lmn*][3,8]phenanthroline-1,3,6,8-tetraone (N5). Mp 145−150 °C; ^{13}C NMR (400 MHz, $CDCl_3$) δ 162.8, 130.4, 126.3, 126.2, 50.0, 32.9, 31.1, 26.2, 22.0, 17.8, 13.5 ppm; ^{1}H NMR (400 MHz, $CDCl_3$) δ 8.71 (s, 4H), 5.26 (m, 2H), 2.18 (m, 2H), 1.92 (m, 2H), 1.58 (d, J = 7.2 Hz, 6H), 1.26 (m, 12H), 0.82 (t, J = 7.5 Hz, 6H) ppm; CI-HRMS (positive ion, M + H^+) calculated for $C_{28}H_{34}N_2O_4$ + H, 463.2597, found 463.2593.

Acknowledgment. We thank Dr. Grant Willson for access to a polarized optical microscope and DSC. We also thank Dr. Jon Sessler for access to a polarized optical microscope. This work was supported by the Robert A. Welch Foundation (F1188) and the National Institutes of Health (GM-069647). Crystallographic data was collected using instrumentation purchased with funds provided by the National Science Foundation, Grant No. 0741973.

Supporting Information Available: Additional experimental information, NMR spectra, UV−vis data for all crystalline mixtures, and crystallographic information files in CIF format. This material is available free of charge via the Internet at http://pubs.acs.org.